

Analysis of the expression, function and signaling of glycogen phosphorylase isoforms in hepatocellular carcinoma

LINGYU JIANG^{1,2}, SHUYAN LIU^{1,2}, TINGZHI DENG^{1,2}, YANG YANG^{1,2} and YIN ZHANG^{1,2}

¹School of Pharmacology; ²Shandong Technology Innovation Center of Molecular Targeting and Intelligent Diagnosis and Treatment, Binzhou Medical University, Yantai, Shandong 264003, P.R. China

Received March 9, 2022; Accepted May 11, 2022

DOI: 10.3892/ol.2022.13364

Abstract. Glycogen phosphorylase (GP) is an essential enzyme for glycolysis via the glycogen degradation pathway. It consists of three isoforms: PYGB (brain form), PYGL (liver form) and PYGM (muscle form). Although the abnormal expression of GP is associated with a variety of tumors, its relationship with hepatocellular carcinoma (HCC) and whether it can be used as a prognostic marker of HCC remains unclear. In the present study, the expression levels of PYGB, PYGL and PYGM were analyzed. It was found that the expression levels of PYGB in tumor tissues were higher than those in normal tissues, particularly in HCC. The high expression of PYGB (hazard ratios=1.801; 95% confidence interval: 1.266-2.562) could predict the poor prognosis of HCC patients but not PYGL and PYGM. Inhibition of PYGB with GP inhibitor CP91149 significantly suppressed the HCC cell proliferation in the HCC cell model. In addition, combination treatment with sorafenib, a standard treatment for HCC, showed a great inhibition on tumor growth and angiogenesis. These findings suggested that PYGB may be used as a therapeutic and prognostic indicator for HCC.

Introduction

Cancer is one of the leading causes of death worldwide. Liver cancer has risen from the third highest cancer-related mortality rate in 2018 to the second highest-related cancer mortality rate in 2020 (1). Globally, liver cancer is the most common fatal malignant tumor. In all cases of liver cancer, more than 90% are hepatocellular carcinoma (HCC) (2). Patients diagnosed for advanced HCC result in poor prognosis. At present, the first-line treatments for advanced HCC are mainly sorafenib-based treatment in combination with

chemotherapy, other targeted therapy, or immunotherapy (3). However, the treatment efficacy remains limited. One problem is that the response rate of sorafenib is significantly low (4). Numerous approaches have been made to improve the drug efficacy, but reliable markers to predict the drug response are still needed. In addition, combination of other anticancer drugs with sorafenib are also widely studied to improve the HCC treatment; for example, targeting cancer metabolism has attracted increasing attention in cancer therapy (5-8).

One of the hallmarks of cancer is the reprogramming of metabolism (9). Cancer cells mainly rely on aerobic glycolysis to maintain cell proliferation. Even in the presence of oxygen, the increase of glucose uptake, also known as 'Warburg effect', is more favorable for cancer cell proliferation (10,11). Glycogen is one of the important glucose sources for cancer cells. It is a high molecular weight branched polysaccharide of glucose, which is the main glucose storage macromolecule in animals. Glycogen stored in liver is essential for maintaining blood glucose level (12). Glycogen phosphorylase (GP) is the key enzyme of glycogen catabolism, which is responsible for the decomposition of glycogen. There are three isoforms of GP: PYGB, PYGL and PYGM (13). GP is activated by phosphorylase kinase and allosteric stimulator glucose-6-phosphate (G6P) at Ser-14. A previous study revealed that the absence of PYGL leads to the increase of reactive oxygen species clusters, cell aging and death (14). In glucose starvation-resistant pancreatic cancer cells, PYGB is a necessary condition for resistance. Inhibition or loss of PYGB leads to cell death (15). Another study also showed that knockdown of PYGB gene significantly inhibits proliferation, invasion and migration of ovarian cancer cells (16). PYGM is usually associated with type V glycogen storage disease, which is a disorder of carbohydrate metabolism in skeleton muscle (17). In the present study, it was demonstrated that PYGB expression was elevated in HCC tumor tissue, which is associated with poor survival in patients with HCC. Clinical data analysis also showed that patients with HCC at late stage have higher PYGB level, which may indicate that PYGB may correlate with the disease progression. Further Gene Ontology (GO) analysis revealed that PYGB is involved in neutrophil activation, cytoplasmic vesicle and coenzyme binding function. Kyoto Encyclopedia of Genes and Genomes (KEGG) analysis indicated that PYGB is involved in insulin signaling, where FBP1, CALM1, CAML2, CAML3 and PHKA2 may have direct interaction with PYGB.

Correspondence to: Dr Yin Zhang or Dr Yang Yang, School of Pharmacology, Binzhou Medical University, 346 Guanhai Road, Yantai, Shandong 264003, P.R. China
E-mail: yin_zhang@bzmc.edu.cn
E-mail: yangyang86@bzmc.edu.cn

Key words: glycogen phosphorylase, PYGB, PYGM, PYGL, hepatocellular carcinoma

Furthermore, in the *in vitro* models, HCC cells were inhibited by a GP inhibitor, CP91149. In the tumor model, combination of CP91149 and sorafenib produced significant tumor suppression effect. Collectively, the present study suggested that glycogen metabolism and GP play important roles in HCC progression and may provide new therapeutic targets for HCC therapy. It may be also possible to combine standard antiangiogenic therapy and anti-metabolism therapy to improve the treatment of HCC.

Materials and methods

Data analysis. The survival curves of PYGB, PYGL, and PYGM in HCC were analyzed by the online data analysis tool GEPIA (<http://gepia.cancer-pku.cn/>) (18). The gene expression in pan-cancer, tumor stage, gene methylation analysis of PYGB, PYGL and PYGM were performed at The University of Alabama at Birmingham Cancer data analysis Portal (19) (UALCAN) (www.ualcan.path.uab.edu/) according to the website instructions. The dataset TCGA-LIHC and TCGA-Pan-cancer from study accession phs000178.v11.p8.v11.p8 (20) was used. The Welch's t-test was used for gene expression analysis in HCC and pan-cancer of PYGB, PYGL and PYGM. The protein 3-D structures were obtained from the Protein Data Bank (PDB) (www.rcsb.org) (21-23). The gene mutation analysis was conducted in cBioportal (www.cbioportal.org) (24,25). The prediction of protein-protein interactions was analyzed in String database (www.string-db.org) (26). The analysis of receiver operating characteristic (ROC) curve, GEO data, GO and KEGG were performed by the online tool Xiantao according to the instructions (<https://www.xiantao.love/products>). The detailed analysis methods are listed below:

UALCAN data analysis for gene expression and clinical clinicopathological factors. The screening conditions set in the present study were: 'Enter gene symbol(s): PYGB, PYGL, or PYGM'; 'TCGA dataset: Liver HCC'; 'Explore'. Results of individual cancer stages, age, sex and tumor grade, methylation and Pan-cancer view will be revealed under each tab. T-test was used for gene expression by the website.

GEPIA data analysis for survival. The screening conditions set in the present study were: 'survival analysis; Gene: PYGB, PYGL, or PYGM'; 'Datasets selection: LIHC'; 'plot'. Log rank test was used for survival by the website.

cBioPortal data analysis for gene mutation. The screening conditions set in the present study were: 'Liver HCC (TCGA, PanCancer Atlas)'; 'query by gene'; 'patient/case set all samples (372)'; 'genes: PYGB, PYGL, or PYGM'; 'submit query'.

STRING data analysis for protein-protein interactions. The screening conditions set in the present study were: 'select Multiple proteins'; 'Gene list: ACACA, ACACB, AKT1, CALM1, CALM2, CALM3, CRKL, EIF4EBP1, FBP1, FOXO1, G6PC, HRAS, PCK1, PCK2, PHKA2, PIK3CD, PIK3R1, PIK3R2, PPP1CA, PPP1CB, PPP1CC, PRKAA1, PRKAB1, PRKAG1, PRKAR1A, PRKAR2A, PRKCI,

PRKCZ, MAPK3, MAPK9, MAP2K1, PYGB, RHEB, RPS6, SREBF1, SOCS2, SOCS3, FLOT1, SORBS1, PPARGC1A, PRKAG2' 'Organism: Homo sapiens'; 'search'.

PDB database for protein structures. The screening conditions set in the present study were: 'PYGB, PYGL, PYGM'; 'Homo sapiens'; 'search'.

Xiantao data analysis for ROC curve. The screening conditions set in the present study were: 'Bioinformatics tools'; 'clinical significance'; 'ROC curve'; 'project: TCGA-LIHC, sample size 424'; 'Gene: PYGB, PYGL and PYGM'; 'confirm'. Website inbuilt R package of pROC (version 1.17.0.1) and ggplot2 package (version 3.3.3) were used to generate the figures. For GO and KEGG analysis. 'Search dataset'; 'GSE84598' (27); 'select tumor or normal samples'; 'Add to database'; 'My database'; 'experiment group: HCC, reference group: normal liver tissue'; 'Analysis'; 'download analysis results'. Genes with adjusted $P < 0.05$ were subjected to GO and KEGG analysis: 'Bioinformatics tools'; 'Function cluster'; 'GO/KEGG analysis'; 'upload'; 'Clustering analysis'; 'GO-BP', 'GO-CC', 'GO-MF', and KEGG options were selected to obtain the analyzed data. Based on these data, genes with adjusted $P < 0.05$ were selected for preparation of the bubble chart under the function of 'GO/KEGG' visualization. Website inbuilt R packages ggplot2 (For bubble chart, version 3.3.3) and clusterProfile (For data analysis, Version 3.14.3) were used. For the univariate and multivariate cox hazard analysis: 'Bioinformatics tools'; 'Univariate/multi-factor cox regression'; 'select TCGA-LIHC, sample size 424, platform RNAseq, format TPM'; 'T stage, pathologic stage, histologic grade, sex, age, PYGB/PYGL/PYGM'; 'confirm'. Website inbuilt R package (survival, version 3.2-10).

Cell culture. Human HCC (MHCC97H) cell line was purchased from Shanghai Yiyan Biological Technology Co., Ltd. Cells were cultured in Dulbecco's Modified Eagle Medium (DMEM) (C11965500BT; Gibco; Thermo Fisher Scientific, Inc.) containing 10% fetal bovine serum (FSP500; Shanghai ExCell Biology, Inc.) and 1% penicillin/streptomycin.

Western blot analysis. MHCC97H cells were lysed in cell lysis buffer (cat. no. P0013; Beyotime Institute of Biotechnology) with protease inhibitors Cocktail (cat. no. B14001; bimake.com). The lysates were purified by centrifugation 4°C at 13,800 x g for 15 min. Protein concentration was determined by Bradford assay. Next, the protein lysates (20 µg) were separated using SDS-PAGE on an 8% gel. Subsequently, samples were separated on polyacrylamide gels and transferred to PVDF membrane, and then blocked with 5% milk at room temperature for 1 h. Membranes were incubated with primary antibodies overnight at 4°C. After washing with TBST, the membranes were incubated with the HRP-conjugated goat polyclonal anti-mouse/rabbit IgG secondary antibody (anti-mouse: cat. no. 115-035-003; anti-rabbit: cat. no. 111-035-003; both 1:5,000; Jackson ImmunoResearch Laboratories, Inc.) was incubated at room temperature for 1 h and processed for western blotting with chemiluminescence detection (cat. no. BL520B; Biosharp Life Sciences). Membranes were incubated with the following primary

antibodies: PYGB (1:1,000; cat. no. AB154969; Abcam), PYGL (1:1,000; cat. no. DF12134; Affinity Biosciences, Ltd.), PYGM (1:1,000; cat. no. 19716-1-AP; ProteinTech Group, Inc.) and β -actin (1:5,000; cat. no. A00702-100; GenScript) were used.

Cell proliferation assay. A total of 1×10^4 cells/well were seeded in a 96-well plate in a 200- μ l culture medium. Cells were placed in the incubator and cultured at 37°C for 12 h. After cells attached to the plate, medium containing CP91149 (25, 50, 75 and 100 μ M) or Sorafenib were added to replace the normal culture medium. After culturing for 48 h, the culture medium was discarded and 100 μ l medium + 10 μ l Cell Counting Kit-8 (cat. no. B34304; bimake.com) were added to each well. After 2 h of incubation in the dark, the OD value was measured under the wavelength of 450 nm by enzyme labeling instrument, and the proliferation rate was measured according to the OD value.

In vivo tumor model. In the *in vivo* study, 33 female nude mice were used to establish the human HCC xenograft tumor model, and finally 6 mice per group were used for the tumor experiment. Mice were purchased from the GemPharmatech. The mice were kept under the following housing conditions: 20–24°C, 40–70% humidity, 12h/12h light/dark cycle, with free access to water and food. The experiment started when the mice were six-week old, and the average of body weight was 19–20 g. To establish the tumor models, 5×10^6 MHCC97H cells in 0.1 ml PBS: Matrigel mix (1:1) were inoculated subcutaneously on the flank of each mouse under anesthesia using isoflurane [cat. no. R510-22; Shenzhen Reward Life Technology Co., Ltd.) (3.0–3.5% for induction and 2.5% for maintenance)]. The drug treatment started when tumor size reached ~ 50 mm³. CP91149 (cat. no. S2717; Selleck Chemicals) at dose of 60 mg/kg per mouse was administered every other day and sorafenib (cat. no. M1827; Abmole Bioscience Inc.) at dose of 60 mg/kg per mouse was administered daily by gavage. The tumor volume was calculated using the following equation: $1/2$ length \times width². Mice were sacrificed by cervical dislocation when the tumor volume was reaching 1,500 mm³. The tumor tissues were harvested and fixed in 4% paraformaldehyde for 24 h at room temperature for further experiments. All animal experiments in the present study were approved (approval no. 2021-201) by the Ethics Committee of Binzhou Medical University (Yantai, China).

Immunohistochemistry. Paraffin sections (4- μ m thick) were incubated at 65°C for 1.5–2 h, followed with deparaffinization in xylene and rehydration in descending ethanol series (99, 95 and 70%). Paraffin sections were then placed in the sodium citrate buffer for antigen retrieval at full power in microwave for 5 min and then 20% power for 30 min. Next, paraffin sections were placed at room temperature for 1 h. Then slides were rinsed in PBS for 5 min \times 3 times. Following incubation with 3% H₂O₂ solution at room temperature for 15 min, sections were then rinsed in PBS for 5 min \times 3 times. Samples were incubated in 0.2% Triton X-100 at room temperature for 10 min, then washed in PBS for 5 min \times 3 times. After washing, paraffin sections were blocked with 5% BSA (cat. no. 9048-46-8; Dalian Meilun Biology Technology Co., Ltd.) at 37°C for 45 min–1 h. Sections were incubated with the primary antibody

KI67 (1:1,000; cat. no. 27309-1-AP; ProteinTech Group, Inc.) at 4°C overnight. On the next day, the paraffin sections were rinsed with PBS for 5 min \times 3 times. Subsequently, sections were incubated with the HRP-conjugated goat anti-rabbit and mouse secondary antibody polymer according to the DAB kit instructions (kit cat. no. GK600510; cat. no. Gene Tech Co., Ltd.) at 37°C for 30–45 min and the paraffin sections were washed with PBS for 5 min \times 3 times. DAB staining solution (kit cat. no. GK600510; Gene Tech Co., Ltd.) was used for the color development of paraffin sections. The paraffins were soaked in hematoxylin solution for 3 min, then rinsed under tap water for 10 min. The sections were differentiated in hydrochloric alcohol for 10 sec, followed by rinsing under tap water for 10 min. The dehydration of sections was performed in the cylinder by the reversed ethanol gradient. The paraffin sections were sealed by the neutral resin and images were captured using a light microscope.

Whole-Mount staining. Briefly, the fixed mouse tumor was cut into thin slices as much as possible. A total of 20 μ g/ml of protease K (cat. no. AG12004; Hunan Aikerui Biological Engineering Co., Ltd.) was added to permeabilize the tissue. Tissues were blocked at 4°C overnight with 3% milk. Then, tissues were incubated with the primary antibody goat anti-mouse CD31 (1:200; AF3628; R&D Systems, Inc.) at 4°C overnight. The samples were incubated with 0.3% Triton X-100 in PBS at 4°C for 1.5 h, then with 3% milk for 1.5 h at room temperature. Subsequently, the samples were incubated with the secondary antibody (donkey anti-goat Alex 555; 1:200; cat. no. A21432; Invitrogen; Thermo Fisher Scientific, Inc.) in the dark for 2 h at room temperature, and then washed again with 1.5% milk for 1 h at room temperature. Samples were washed with 0.3% Triton X-100 in PBS at 4°C overnight and tissues were mounted with anti-fluorescence quenching agent. Images were captured using a confocal microscope.

Statistical analysis. The statistics for *in vitro* and *in vivo* experiments were performed using ANOVA followed by Dunnett's post hoc test. Data were presented as the mean \pm SEM. $P < 0.05$ was considered to indicate a statistically significant difference. Statistical analysis was performed using GraphPad Prism version 9.3.1 (471) (GraphPad Software, Inc.).

Results

Expression of PYGB, PYGL and PYGM in cancer. To evaluate the general expression pattern of GPs, the expression of the three GPs was compared in different types of cancer to obtain a general expression pattern. The database UALCAN was used to analyze the mRNA expression of PYGB, PYGL and PYGM in tumor and normal tissues. The results showed that PYGB expression levels were significantly higher in liver HCC (LIHC) compared with other types of cancer. In addition, there was an increase of PYGB expression in the HCC compare with normal liver tissue (Fig. S1A). PYGL expression level was depending on different types of cancer, where there were no significant changes of PYGL in LIHC (Fig. S1B). Notably, most types of cancer had markedly low PYGM expression (Fig. S1C). These data showed that PYGB and PYGL are relatively high expressed, whereas PYGM is low expressed in

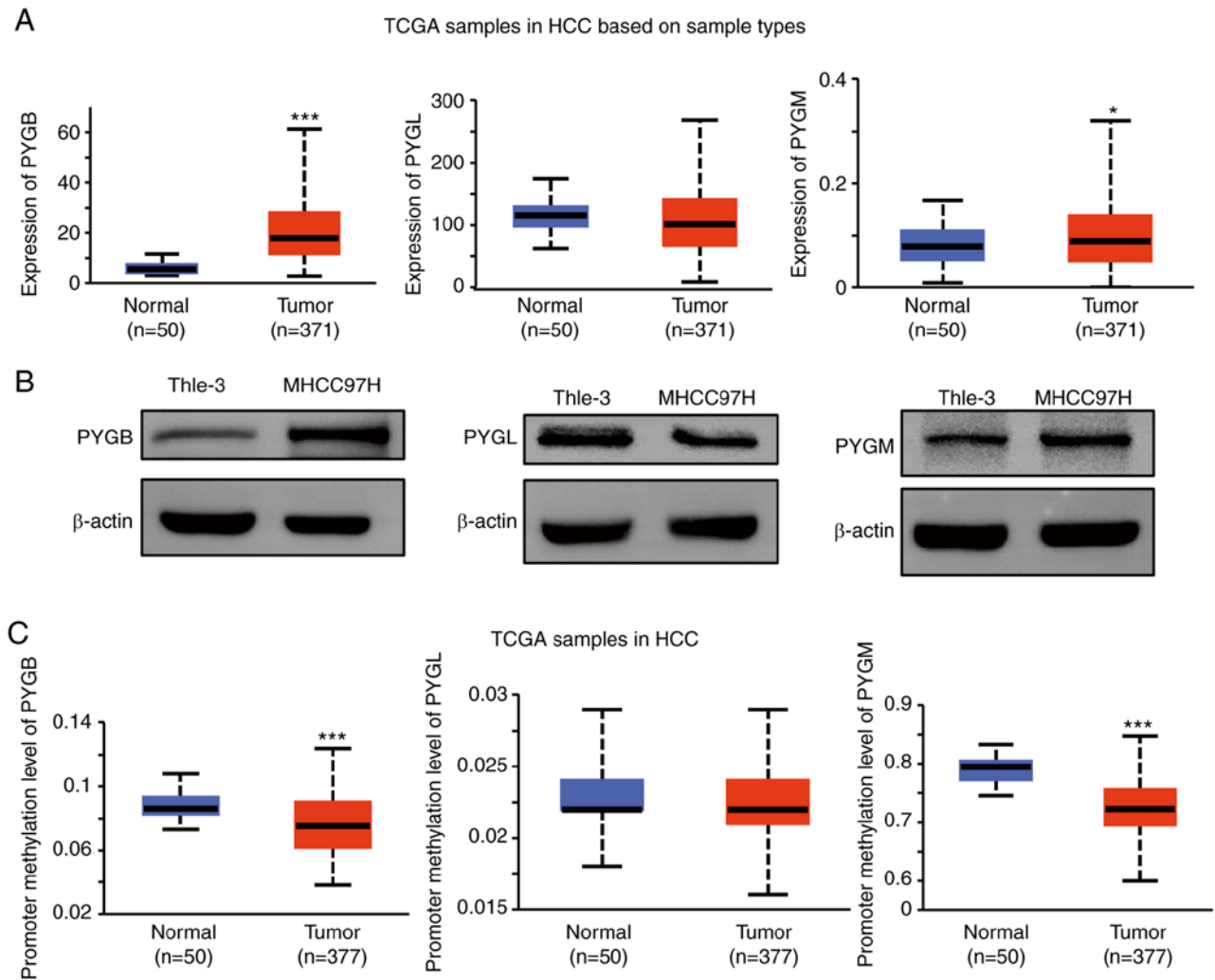


Figure 1. Analysis of the expression of PYGB, PYGL and PYGM in HCC. (A) Analysis of PYGB, PYGL and PYGM mRNA expression in HCC from UALCAN (<http://ualcan.path.uab.edu/analysis.html>). Dataset TCGA-LIHC from study accession phs000178.v11.p8 was used. (B) Analysis of PYGB, PYGL and PYGM protein expression in a human HCC cell line (MHCC97H) by western blotting. (C) Promoter methylation level analysis of PYGB, PYGL and PYGM in HCC from UALCAN. The dataset TCGA-LIHC from study accession phs000178.v11.p8 was used. * $P < 0.05$, *** $P < 0.001$. PYGB, brain isoform of glycogen phosphorylase; PYGL, liver form of glycogen phosphorylase; PYGM, muscle form of glycogen phosphorylase; HCC, hepatocellular carcinoma; TCGA-LIHC, The Cancer Genome Atlas-liver hepatocellular carcinoma.

most types of cancer. In HCC, PYGB is significantly increased in tumor tissue, whereas PYGL had no differences and PYGM showed a nearly detectable expression. This data indicated that PYGB may play an important role in HCC.

The expression of PYGB, PYGL and PYGM in HCC. As the expression of PYGB mRNA was increased in HCC tissue (Fig. 1A), the protein expression in HCC cells was investigated. PYGB, PYGL, and PYGM were analyzed in a human HCC cell line (MHCC97H). Western blot analysis confirmed the high expression of PYGB in a human HCC cell line, but not PYGL or PYGM (Fig. 1B). As the gene methylation may be involved in the phosphorylase expression levels, the methylation level on these isoforms in HCC was explored. Compared with normal tissues, methylation levels of PYGB and PYGM are significantly lower in tumor tissues. However, there was no significant difference of PYGL between tumor tissues and normal tissues (Fig. 1C). These data indicated that the high PYGB expression may be due to the low methylation level, which also implies that

epigenetic regulation may play a role in PYGB gene expression.

Gene alterations in PYGB, PYGL and PYGM in HCC. Since there are few studies on GP in HCC, the present study focused on the analysis in HCC. The natural 3D structures of the three isoforms of GPs, retrieved from PDB database, were compared. Although these isoforms share similar DNA sequences, the protein structures are not exactly the same, indicating a slight activity difference of PYGB, PYGL and PYGM (Fig. S2A). PYGB, PYGL and PYGM were found to have mutations of 0.5, 0.5 and 1.3% of the sequenced cases, respectively (data obtained from the OncoPrint schematic of cBioPortal; Fig. S2B). The data showed that these mutations include missense mutation, truncating mutation, amplification and deep deletion. The overall alteration frequency is ~2.5%, consisting of mutation, amplification and other multiple alterations (Fig. S2B). Further analysis showed the mutations in these 3 isoforms. PYGM has 5 mutation sites, whereas both PYGL and PYGB have only one mutation site (Fig. 2C). These

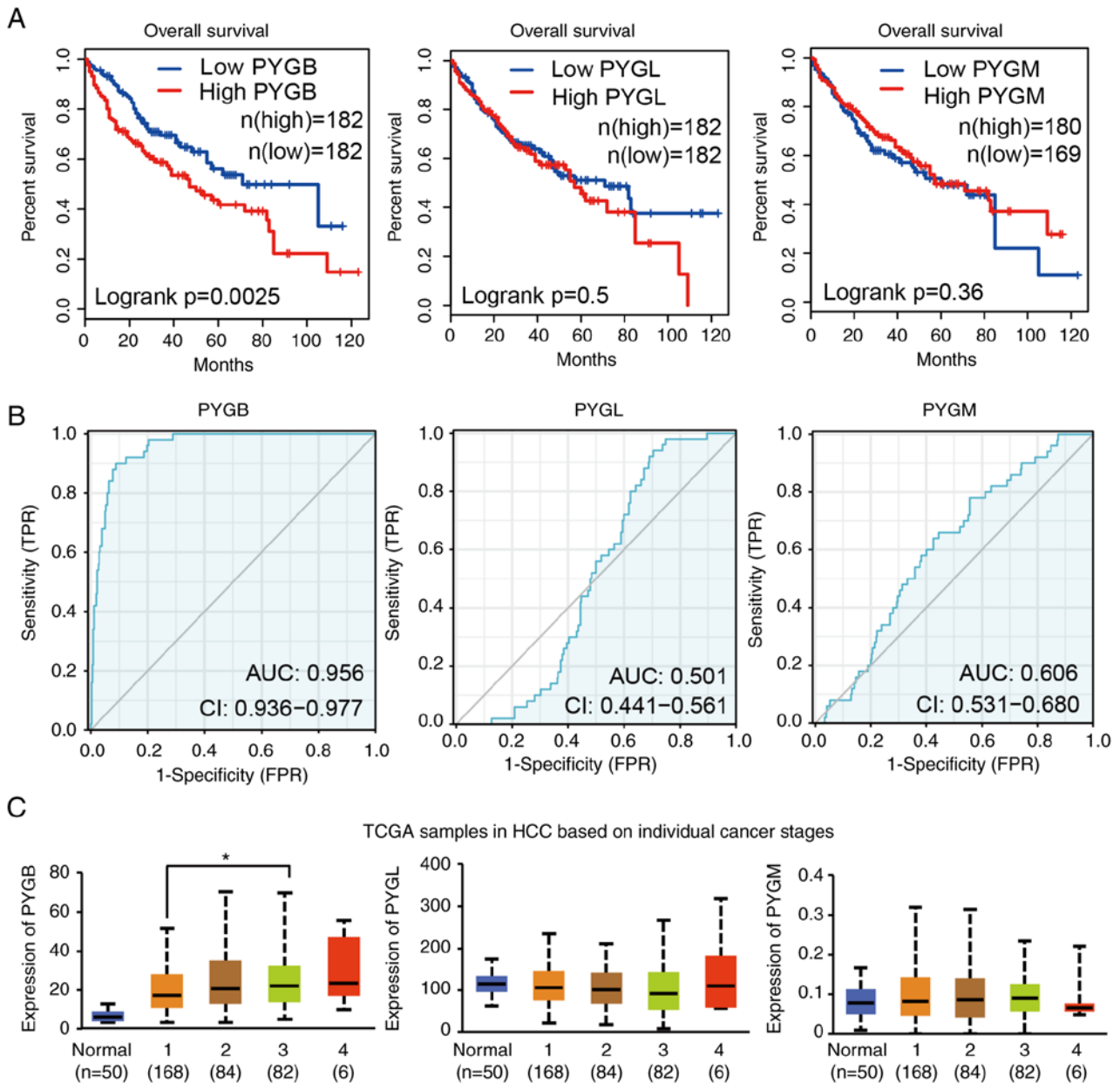


Figure 2. Analysis of the association between GPs and clinicopathological factors in HCC. (A) Survival analysis of expression of GP isoforms in patients with HCC. (B) The receiver operating characteristic curve analysis of PYGB, PYGL and PYGM respectively using the online analysis tool Xiantao. (C) Association between PYGB, PYGL and PYGM expression and cancer stages in HCC. The dataset TCGA-LIHC from study accession phs000178.v11.p8 was used for A-C. * $P < 0.05$. GP, glycogen phosphorylase; PYGB, brain isoform of glycogen phosphorylase; PYGL, liver form of glycogen phosphorylase; PYGM, muscle form of glycogen phosphorylase; HCC, hepatocellular carcinoma; The Cancer Genome Atlas-liver hepatocellular carcinoma.

results indicated that GPs are quite conserved in structure and they have stable functions.

Association of PYGB, PYGL, and PYGM expression with clinicopathological factors in HCC. To explore the relation between GPs and the prognosis of patients with HCC, survival of patients with high or low GP expression was analyzed by GEPIA. It was identified that patients with high PYGB expression had poor survival, but the high expression of PYGL and PYGM had no effect on the survival of patients with HCC (Fig. 2A). By using the ROC curve, the distinguishing efficacy of PYGB, PYGL and PYGM between HCC tissues and normal liver tissue was analyzed. The area under the curve (AUC) of PYGB was 0.956, suggesting that PYGB

may be a potentially marker for prognosis of patients with HCC (Fig. 2B), but not PYGL or PYGM. Analysis of patient individual cancer stage revealed that the PYGB expression are markedly higher in stage 1-4 [stage classification is based on American Joint Committee on Cancer pathologic tumor stage information (19)]. There was also a trend that PYGB expression increases along with the stage. PYGB expression in stage 3 showed a significant increase compared with stage 1. Although stage 4 exhibited the highest PYGB expression, but it did not reach statistically significant difference, which may be due to the small number of samples (Fig. 2C). However, PYGL and PYGM expression did not exhibit significant changes. Additionally, PYGB expression was the only isoform to be increased with age of patients, but not PYGL or PYGM

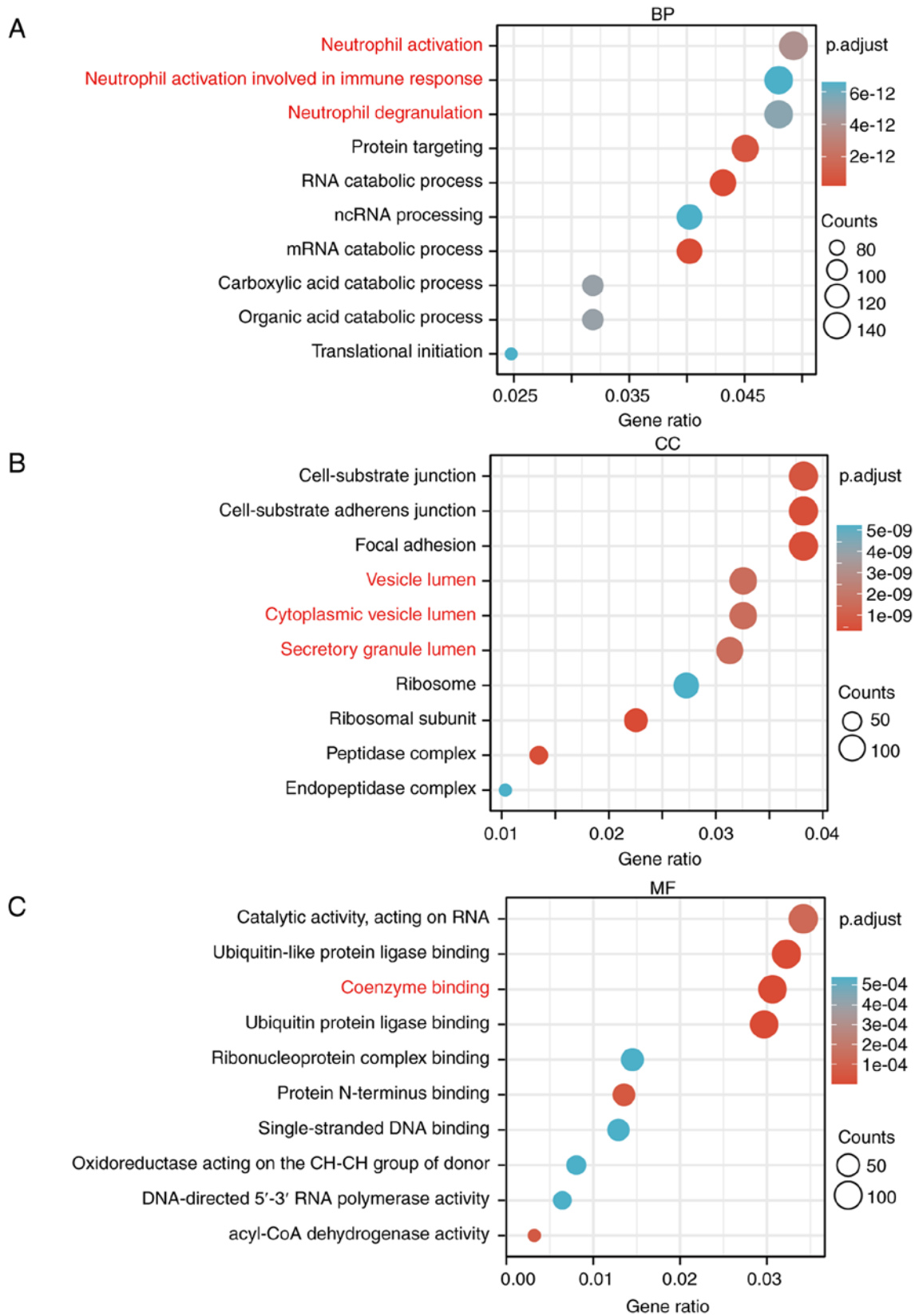


Figure 3. Gene Ontology enrichment analysis using the online analysis tool Xiantao predicted the functional roles of the target host gene PYGB from three aspects: (A) BP process, (B) CC and (C) MF. The dataset used was retrieved from GEO (dataset GSE84598). PYGB, brain isoform of glycogen phosphorylase; BP, biological process; CC, cellular component; MF, molecular function.

(Fig. S3A). The sex did not show any association with the expression of PYGB, PYGL, or PYGM (Fig. S3B). Regarding the tumor grade, PYGB expression increased in all the grades,

whereas PYGL decreased in stage 4 and no changes were found in PYGM expression (Fig. S3C). To analyze if GP could predict the prognosis of patients with HCC, univariate

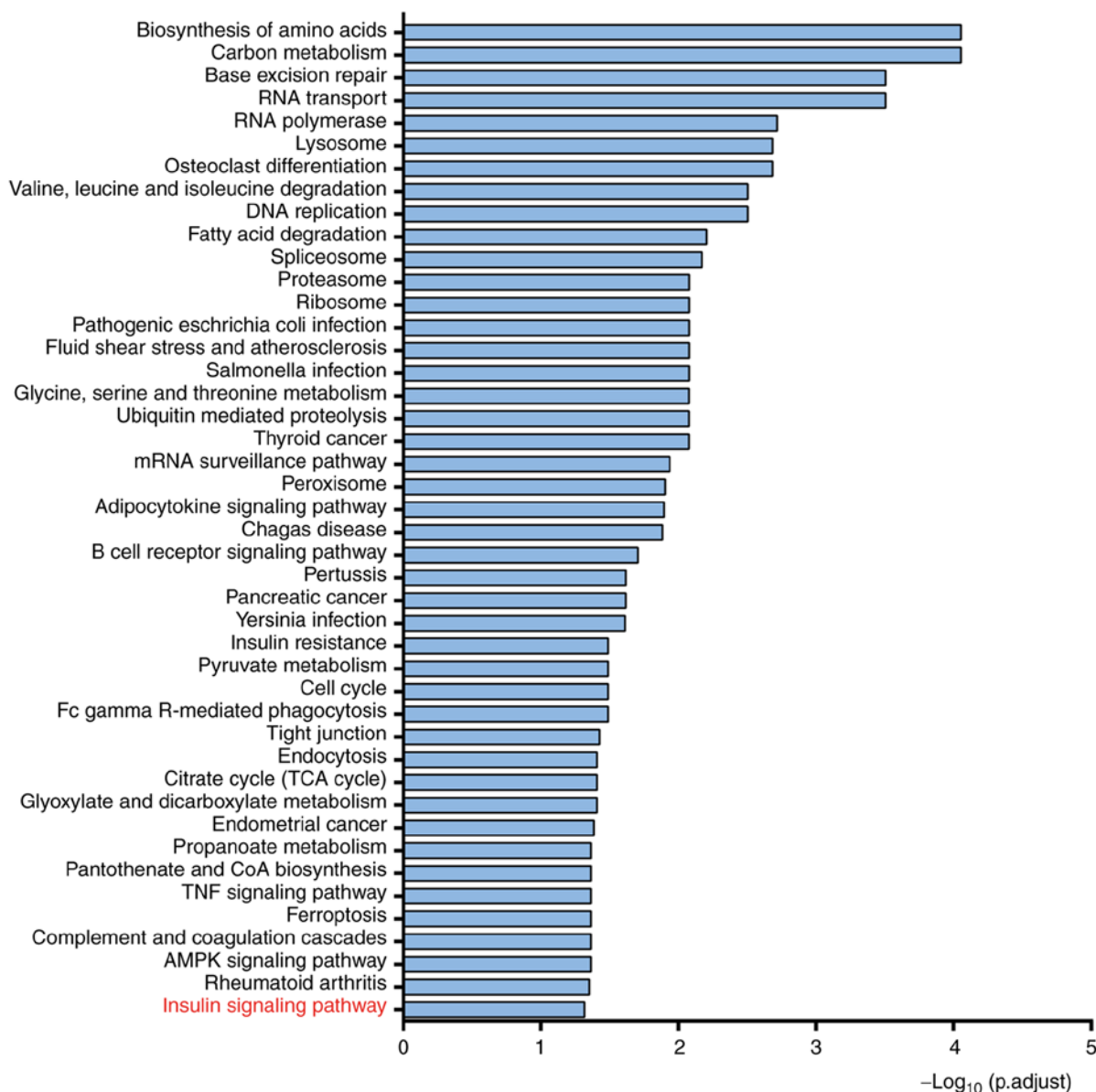


Figure 4. KEGG analysis of the PYGB-involved signaling pathway using the online analysis tool Xiantao. The dataset used was retrieved from GEO (dataset GSE84598). PYGB, brain isoform of glycogen phosphorylase.

and multivariate cox hazard analysis was applied for PYGB, PYGL and PYGM. The data showed that only PYGB reached statistical significance in associating with prognosis of patients (Table SI). These data demonstrated that PYGB is associated with poor survival in patients with HCC and high level of PYGB may indicate a poor prognosis.

Go and KEGG analysis of PYGB in HCC datasets. The HCC dataset GSE84598 from GEO database was analyzed, among which normal liver tissues as well as HCC tissues were selected for KEGG analysis and GO enrichment analysis, including biological process, cellular component and molecular function. A total of 4609 genes from 12581 genes were obtained by adjusting $P < 0.05$. Biological process analysis identified that PYGB is involved in neutrophil activation and degranulation. Cellular components analysis revealed that PYGB participates in vesicle lumen, cytoplasmic vesicle lumen, and secretory granule lumen. Molecular function analysis revealed that

PYGB is involved in coenzyme binding (Fig. 3A-C). KEGG analysis found that PYGB may regulate the insulin signaling pathway (Fig. 4). These data suggested possible functions, biological process and signaling pathways where PYGB plays a role. These results needed to be further validated in both *in vitro* and *in vivo* models.

Gene regulatory network is directly related to PYGB in insulin signaling pathway. Further analysis using String identified 41 proteins that play a role in the insulin signaling pathway involved in regulation by PYGB; and five that are directly related to PYGB were CALM1, CALM2, CALM3, PHKA2 and FBP1 (Fig. 5). CALM1-3 as well as PHKA2 both belong to phosphatase kinases (28,29). CALM1-3 is a calmodulin that mediates the control of a large number of enzymes, ion channels, aquaporins and other proteins through calcium binding. Among the calmodulin calcium complex-stimulated enzymes are a number of protein kinases

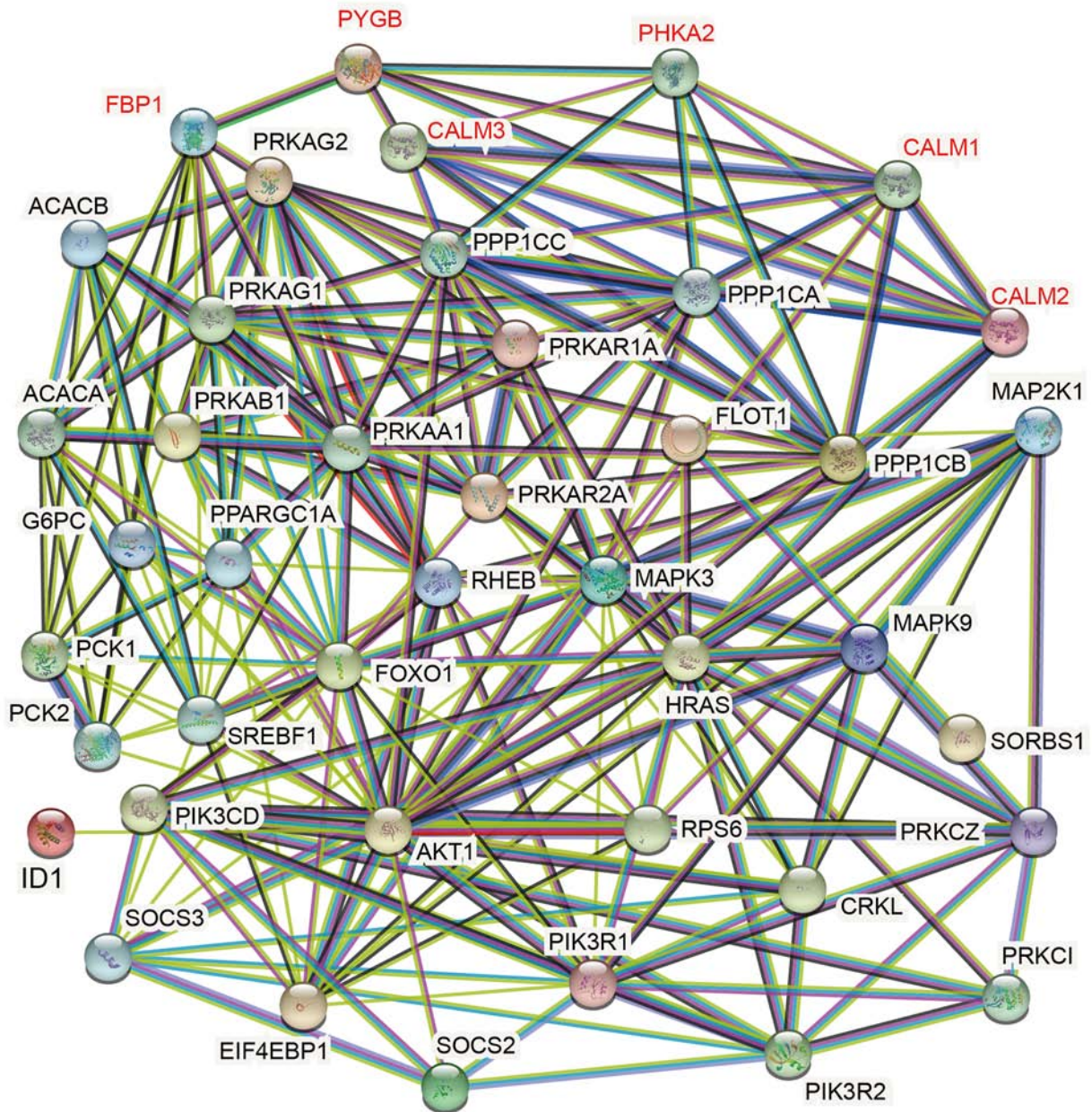


Figure 5. Protein interaction analysis of PYGB-related genes in the insulin signaling pathway from String database. The dataset used to select insulin related genes was retrieved from GEO (dataset GSE84598). Red marked genes are directly related to PYGB. PYGB, brain isoform of glycogen phosphorylase.

and phosphatases (28,30); PHKA2 is a phosphorylase b kinase that catalyzes the phosphorylation of serine in certain substrates. α chain can bind Calmodulin (29). FBP1, the rate limiting enzyme in gluconeogenesis, catalyzes the hydrolysis of fructose 1,6-bisphosphate to sugar 6-phosphate in the presence of divalent cations and plays a role in regulating glucose sensing and insulin secretion of pancreatic β -cells and appears to regulate gluconeogenesis from glycerol in the liver (31), but the specific mechanism in which PYGB acts needs to be validated by further studies.

Inhibition of PYGB activity suppresses HCC growth. To verify the role in PYGB in HCC development, the compound CP91149 was used, which can inhibit GP activity (32) to treat the human HCC cell line MHCC97H. As revealed in Fig. 6A, CP91149 could significantly suppress HCC viability

in a dose-dependent manner. As sorafenib is widely used for HCC treatment, sorafenib was also combined with CP91149 to examine if there would be a synergistic antitumor effect. Indeed, the combination therapy produced increasing significant inhibition on HCC along with the CP91149 dose gradient (Fig. 6B). Next, the result was further validated in the xenograft mouse tumor model with the human HCC cell line MHCC97H. Vehicle, CP91149 (60 mg/kg), sorafenib (60 mg/kg) and sorafenib + CP91149 were administered to the tumor-bearing mice when the tumor started to increase in size. Combination therapy increased tumor inhibition effect compared with control or single drug treatment (Fig. 6C-E). Sorafenib at 60 mg/kg did not show tumor inhibition, as usually the dose at 100 mg/kg can suppress tumors (33) in similar settings (34). Similarly, CP91149 produced no tumor inhibition effect, which may be due to insufficient

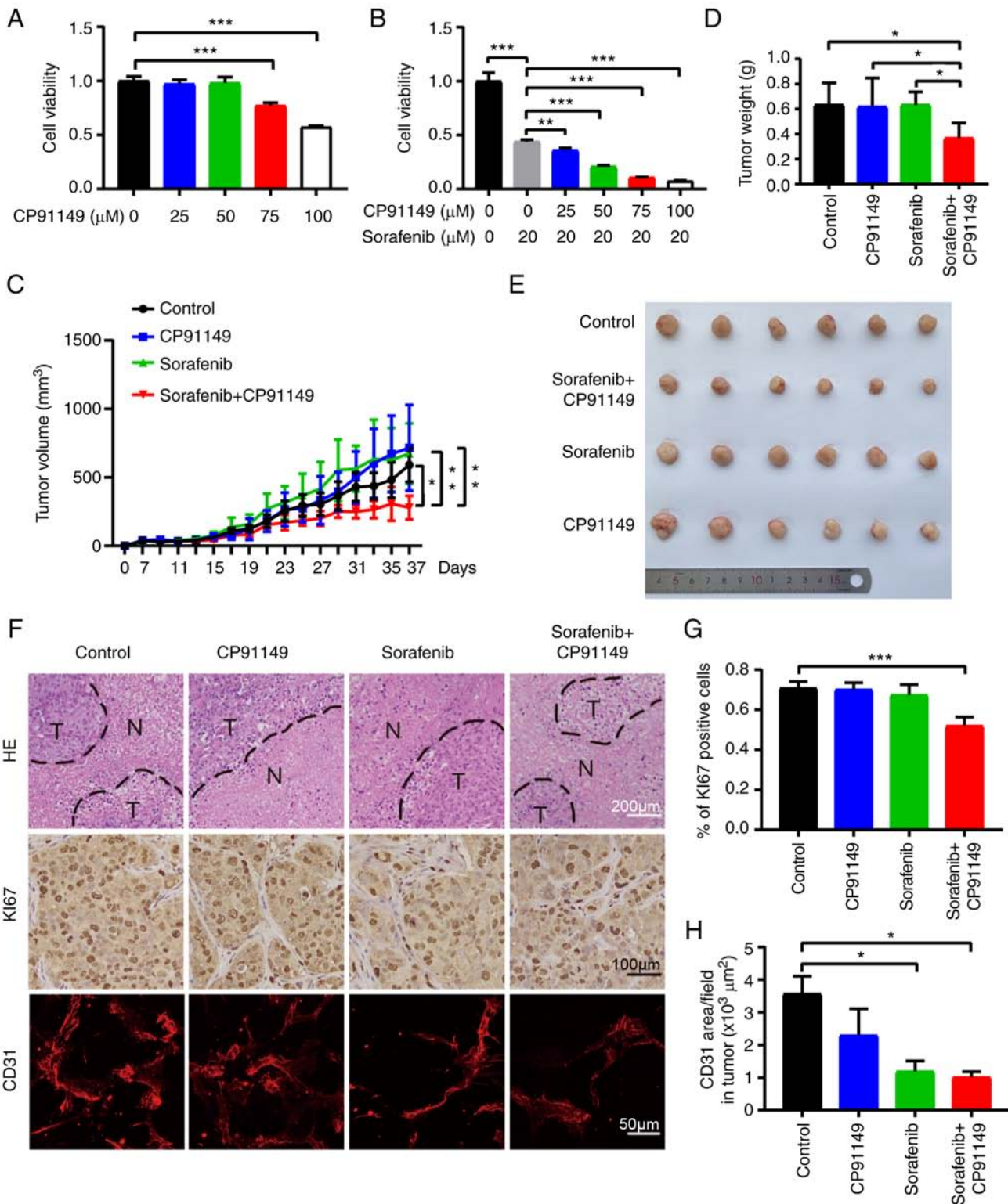


Figure 6. Inhibition of PYGB suppresses HCC growth. (A) HCC cell viability analysis of CP91149 treatment. (B) HCC cell viability analysis of CP91149 treatment combined with sorafenib. (C) Tumor growth curve of HCC under vehicle (n=6), CP91149 (n=6), sorafenib (n=6), or combination treatment (n=6). (D) HCC tumor weight. (E) HCC tumor pictures. (F) H&E (scale bar, 200 μm) staining of tumor tissues and immunohistochemical analysis of Ki67 (scale bar, 100 μm) and CD31 (scale bar, 50 μm). (G) Quantification of Ki67 positive cells. (H) Quantification of blood vessel density. *P<0.05, **P<0.01 and ***P<0.001. N, necrotic tissue; T, tumor tissue; n, number of mice; PYGB, brain isoform of glycogen phosphorylase; HCC, hepatocellular carcinoma.

effectiveness of the dose used. As there are no studies on the effectiveness of CP91149 on HCC tumors, further investigations of the dose effect are needed. Differences in terms of necrotic area changes in tumor tissues were not revealed using H&E staining. However, immunohistochemical

analysis showed that the proliferation marker of Ki67 was decreased in the combination treatment group compared with the control group, which is consistent with the tumor growth and tumor weight (Fig. 6F and G). Surprisingly, the CP91149-treated tumor showed a trend of decreased blood

vessel density, where the combination treatment largely suppressed vessels. This result indicated that CP91149 may have potential to induce the inhibition of tumor angiogenesis, and the combination treatment may further inhibit blood vessels (Fig. 6F and H). Although mono-treatment of either sorafenib or CP91149 did not produce tumor inhibition, however, the combination showed significant tumor suppression. This phenomenon indicates that there may be a synergistic effect due to the inhibition of glycogen metabolism by CP91149 and tumor angiogenesis by sorafenib even at relatively low dose. Taken together, all the aforementioned data indicated that PYGB plays an important role in HCC growth, and it may be developed as a therapeutic target for treatment of HCC.

Discussion

HCC is one of the major causes of death among other cancer-related mortality. Current treatments for advanced HCC have limited benefits in improving the survival of patients (35,36). Targeting cancer cell metabolism is one of the promising directions for anticancer drug development, as an increasing number of studies have revealed the key roles of glucose and lipid in regulating cancer cell proliferation and metastasis (37,38). Glucose is the major source of energy for cancer cells, and glycolysis produces not only energy, but also essential substrates for cancer cells to synthesize materials for cell proliferation, as well as maintaining a favorable tumor microenvironment (39-41). Although cancer cells uptake glucose from blood, the glycogen stored in cells is also an important source to balance the glucose level. Studies have demonstrated that the process of degradation of glycogen into glucose is also significantly involved in cancer cell metabolism through the GP (42-45). Numerous studies have reported that overexpression of GP promotes cancer cell proliferation and metastasis in different types of cancer (46-48), and further studies also proposed several inhibitors for drug development. However, there is no approved drug available at present, thus further investigations are needed.

In the present study, the expression of 3 GP isoforms in different types of cancer were systematically analyzed using UALCAN databases. PYGB and PYGL exhibited increased expression in numerous types of cancer whereas PYGM expression remained unchanged or decreased. The comparison of the structures showed a very conserved protein sequence indicating the similar functions. Nevertheless, the 3D structures also imply the activity difference. It was found that among these 3 GPs, PYGB has low DNA methylation level in HCC, accompanied with significantly elevated expression. Survival curve also showed an association of PYGB expression with poor survival rate. Clinical classification also revealed that PYGB expression increases along with the disease progression, but not the other two isoforms. Further analysis identified certain potential molecules in connection with the PYGB pathway and signaling in HCC. These data demonstrated that PYGB may play an important role in regulation of HCC development. In the validation experiments, the present data showed that inhibition of PYGB activity could suppress HCC cell viability. Although the compound CP91149 did not reach significance

due to dose issues, the combination of PYGB inhibitor and sorafenib greatly retarded tumor growth and tumor angiogenesis. Therefore, targeting PYGB may be a new approach in the treatment of HCC.

Acknowledgements

Not applicable.

Funding

The present study was supported by Taishan Scholar's program of Shandong Provincial Natural Science Foundation (grant no. ZR2021MH292), the National Natural Science Foundation of China (grant no. 82103391) and the Youth Science Foundation project of Shandong Province Natural Science Foundation (grant no. ZR2020QH242).

Availability of data and materials

The datasets used and analyzed during the current study are available from the corresponding author on reasonable request.

Authors' contributions

YZ generated the ideas and designed experiments. LJ, SL and TD performed the database analysis, and the cell and animal experiments. YY supervised the *in vivo* assays. YZ, YY and LJ analyzed the data, organized the figures, and wrote the manuscript. All authors read and approved the final manuscript. YY and LJ confirm the authenticity of all the raw data.

Ethics approval and consent to participate

All animal experiments in the present study were approved by the Ethics Committee of Binzhou Medical University (Yantai, China).

Patient consent for publication

Not applicable.

Competing interests

The authors declare that they have no competing interests.

References

1. Cao W, Chen HD, Yu YW, Li N and Chen WQ: Changing profiles of cancer burden worldwide and in China: A secondary analysis of the global cancer statistics 2020. *Chin Med J (Engl)* 134: 783-791, 2021.
2. Anwanwan D, Singh SK, Singh S, Saikam V and Singh R: Challenges in liver cancer and possible treatment approaches. *Biochim Biophys Acta Rev Cancer* 1873: 188314, 2020.
3. Kudo M: Systemic therapy for hepatocellular carcinoma: 2017 update. *Oncology* 93 (Suppl 1): 135-146, 2017.
4. Shao YY, Hsu CH and Cheng AL: Predictive biomarkers of sorafenib efficacy in advanced hepatocellular carcinoma: Are we getting there? *World J Gastroenterol* 21: 10336-10347, 2015.
5. Mossenta M, Busato D, Dal Bo M and Toffoli G: Glucose metabolism and oxidative stress in hepatocellular carcinoma: Role and possible implications in novel therapeutic strategies. *Cancers (Basel)* 12: 1668, 2020.

6. Lai Y, Huang H, Abudoureyimu M, Lin X, Tian C, Wang T, Chu X and Wang R: Non-coding RNAs: Emerging regulators of glucose metabolism in hepatocellular carcinoma. *Am J Cancer Res* 10: 4066-4084, 2020.
7. Li Z and Zhang H: Reprogramming of glucose, fatty acid and amino acid metabolism for cancer progression. *Cell Mol Life Sci* 73: 377-392, 2016.
8. Hay N: Reprogramming glucose metabolism in cancer: Can it be exploited for cancer therapy? *Nat Rev Cancer* 16: 635-649, 2016.
9. Hanahan D and Weinberg RA: Hallmarks of cancer: The next generation. *Cell* 144: 646-674, 2011.
10. Lunt SY and Vander Heiden MG: Aerobic glycolysis: Meeting the metabolic requirements of cell proliferation. *Annu Rev Cell Dev Biol* 27: 441-464, 2011.
11. Warburg O: On the origin of cancer cells. *Science* 123: 309-314, 1956.
12. Praly JP and Vidal S: Inhibition of glycogen phosphorylase in the context of type 2 diabetes, with focus on recent inhibitors bound at the active site. *Mini Rev Med Chem* 10: 1102-1126, 2010.
13. Agius L: Role of glycogen phosphorylase in liver glycogen metabolism. *Mol Aspects Med* 46: 34-45, 2015.
14. Favaro E, Bensaad K, Chong MG, Tennant DA, Ferguson DJ, Snell C, Steers G, Turley H, Li JL, Günther UL, *et al*: Glucose utilization via glycogen phosphorylase sustains proliferation and prevents premature senescence in cancer cells. *Cell Metab* 16: 751-764, 2012.
15. Philips KB, Kurtoglu M, Leung HJ, Liu H, Gao N, Lehrman MA, Murray TG and Lampidis TJ: Increased sensitivity to glucose starvation correlates with downregulation of glycogen phosphorylase isoform PYGB in tumor cell lines resistant to 2-deoxy-D-glucose. *Cancer Chemother Pharmacol* 73: 349-361, 2014.
16. Zhou Y, Jin Z and Wang C: Glycogen phosphorylase B promotes ovarian cancer progression via Wnt/ β -catenin signaling and is regulated by miR-133a-3p. *Biomed Pharmacother* 120: 109449, 2019.
17. de Luna N, Brull A, Guiu JM, Lucia A, Martin MA, Arenas J, Martí R, Andreu AL and Pinós T: Sodium valproate increases the brain isoform of glycogen phosphorylase: Looking for a compensation mechanism in McArdle disease using a mouse primary skeletal-muscle culture in vitro. *Dis Model Mech* 8: 467-472, 2015.
18. Tang Z, Li C, Kang B, Gao G, Li C and Zhang Z: GEPIA: A web server for cancer and normal gene expression profiling and interactive analyses. *Nucleic Acids Res* 45(W1): W98-W102, 2017.
19. Chandrashekar DS, Bashel B, Balasubramanya SAH, Creighton CJ, Ponce-Rodriguez I, Chakravarthi B VSK and Varambally S: UALCAN: A portal for facilitating tumor subgroup gene expression and survival analyses. *Neoplasia* 19: 649-658, 2017.
20. Cancer Genome Atlas Research Network: Comprehensive genomic characterization defines human glioblastoma genes and core pathways. *Nature* 455: 1061-1068, 2008.
21. Rath VL, Ammirati M, LeMotte PK, Fennell KF, Mansour MN, Danley DE, Hynes TR, Schulte GK, Wasilko DJ and Pandit J: Activation of human liver glycogen phosphorylase by alteration of the secondary structure and packing of the catalytic core. *Mol Cell* 6: 139-148, 2000.
22. Lukacs CM, Oikonomakos NG, Crowther RL, Hong LN, Kammlott RU, Levin W, Li S, Liu CM, Lucas-McGady D, Pietranico S and Reik L: The crystal structure of human muscle glycogen phosphorylase a with bound glucose and AMP: An intermediate conformation with T-state and R-state features. *Proteins* 63: 1123-1126, 2006.
23. Mathieu C, Li de la Sierra-Gallay I, Duval R, Xu X, Cacaig A, Léger T, Woffendin G, Camadro JM, Etchebest C, Haouz A, *et al*: Insights into Brain glycogen metabolism: The structure of human brain glycogen phosphorylase. *J Biol Chem* 291: 18072-18083, 2016.
24. Gao J, Aksoy BA, Dogrusoz U, Dresdner G, Gross B, Sumer SO, Sun Y, Jacobsen A, Sinha R, Larsson E, *et al*: Integrative analysis of complex cancer genomics and clinical profiles using the cBioPortal. *Sci Signal* 6: pii, 2013.
25. Cerami E, Gao J, Dogrusoz U, Gross BE, Sumer SO, Aksoy BA, Jacobsen A, Byrne CJ, Heuer ML, Larsson E, *et al*: The cBio cancer genomics portal: An open platform for exploring multidimensional cancer genomics data. *Cancer Discov* 2: 401-404, 2012.
26. Jensen LJ, Kuhn M, Stark M, Chaffron S, Creevey C, Muller J, Doerks T, Julien P, Roth A, Simonovic M, *et al*: STRING 8-a global view on proteins and their functional interactions in 630 organisms. *Nucleic Acids Res* 37 (Database issue): D412-D416, 2009.
27. Castven D, Fischer M, Becker D, Heinrich S, Andersen JB, Strand D, Sprinzl MF, Strand S, Czauderna C, Heilmann-Heimbach S, *et al*: Adverse genomic alterations and stemness features are induced by field cancerization in the microenvironment of hepatocellular carcinomas. *Oncotarget* 8: 48688-48700, 2017.
28. Chin D and Means AR: Calmodulin: A prototypical calcium sensor. *Trends Cell Biol* 10: 322-328, 2000.
29. Fu J, Wang T and Xiao X: A novel PHKA2 mutation in a Chinese child with glycogen storage disease type IXa: A case report and literature review. *BMC Med Genet* 20: 56, 2019.
30. Tsang WY, Spektor A, Luciano DJ, Indjeian VB, Chen Z, Salisbury JL, Sánchez I and Dynlacht BD: CP110 cooperates with two calcium-binding proteins to regulate cytokinesis and genome stability. *Mol Biol Cell* 17: 3423-3434, 2006.
31. Kebede M, Favaloro J, Gunton JE, Laybutt DR, Shaw M, Wong N, Fam BC, Aston-Mourney K, Rantza C, Zulli A, *et al*: Fructose-1,6-bisphosphatase overexpression in pancreatic beta-cells results in reduced insulin secretion: A new mechanism for fat-induced impairment of beta-cell function. *Diabetes* 57: 1887-1895, 2008.
32. Rocha S, Lucas M, Araujo AN, Corvo ML, Fernandes E and Freitas M: Optimization and validation of an in vitro standardized glycogen phosphorylase activity assay. *Molecules* 26: 4635, 2021.
33. Caiola E, Frapolli R, Tomanelli M, Valerio R, Iezzi A, Garassino MC, Broggin M and Marabese M: Weel inhibitor MK1775 sensitizes KRAS mutated NSCLC cells to sorafenib. *Sci Rep* 8: 948, 2018.
34. Qu Z, Wu J, Wu J, Luo D, Jiang C and Ding Y: Exosomes derived from HCC cells induce sorafenib resistance in hepatocellular carcinoma both in vivo and in vitro. *J Exp Clin Cancer Res* 35: 159, 2016.
35. Li S, Yang F and Ren X: Immunotherapy for hepatocellular carcinoma. *Drug Discov Ther* 9: 363-371, 2015.
36. Lurje I, Czigan Z, Bednarsch J, Roderburg C, Isfort P, Neumann UP and Lurje G: Treatment strategies for hepatocellular carcinoma: a multidisciplinary approach. *Int J Mol Sci* 20: 1465, 2019.
37. Luengo A, Gui DY and Vander Heiden MG: Targeting metabolism for cancer therapy. *Cell Chem Biol* 24: 1161-1180, 2017.
38. Bose S, Zhang C and Le A: Glucose metabolism in cancer: The Warburg effect and beyond. *Adv Exp Med Biol* 1311: 3-15, 2021.
39. Abdel-Wahab AF, Mahmoud W and Al-Harizy RM: Targeting glucose metabolism to suppress cancer progression: Prospective of anti-glycolytic cancer therapy. *Pharmacol Res* 150: 104511, 2019.
40. Gomes AS, Ramos H, Soares J and Saraiva L: p53 and glucose metabolism: An orchestra to be directed in cancer therapy. *Pharmacol Res* 131: 75-86, 2018.
41. Ancy PB, Contat C and Meylan E: Glucose transporters in cancer-from tumor cells to the tumor microenvironment. *FEBS J* 285: 2926-2943, 2018.
42. Zois CE and Harris AL: Glycogen metabolism has a key role in the cancer microenvironment and provides new targets for cancer therapy. *J Mol Med (Berl)* 94: 137-154, 2016.
43. Ritterson Lew C, Guin S and Theodorescu D: Targeting glycogen metabolism in bladder cancer. *Nat Rev Urol* 12: 383-391, 2015.
44. Zois CE, Favaro E and Harris AL: Glycogen metabolism in cancer. *Biochem Pharmacol* 92: 3-11, 2014.
45. Favaro E and Harris AL: Targeting glycogen metabolism: A novel strategy to inhibit cancer cell growth? *Oncotarget* 4: 3-4, 2013.
46. Jin Y and Yang Y: Bioinformatics-based discovery of PYGM and TNNC2 as potential biomarkers of head and neck squamous cell carcinoma. *Biosci Rep* 39: BSR20191612, 2019.
47. Altemus MA, Goo LE, Little AC, Yates JA, Cheriyan HG, Wu ZF and Merajver SD: Breast cancers utilize hypoxic glycogen stores via PYGB, the brain isoform of glycogen phosphorylase, to promote metastatic phenotypes. *PLoS One* 14: e0220973, 2019.
48. Xia B, Zhang K and Liu C: PYGB promoted tumor progression by regulating Wnt/ β -catenin pathway in gastric cancer. *Technol Cancer Res Treat* 19: 1533033820926592, 2020.

